Molecular Biology of the Cell
Vol. 20, 2722–2730, June 1, 2009

Kinesin-1 and Cytoplasmic Dynein Act Sequentially to Move the Meiotic Spindle to the Oocyte Cortex in *Caenorhabditis elegans*

Marina L. Ellefson and Francis J. McNally

Department of Molecular and Cellular Biology, University of California, Davis, Davis, CA 95616

Submitted January 2, 2009; Revised March 12, 2009; Accepted March 27, 2009
Monitoring Editor: Tim Stearns

During female meiosis in animals, the meiotic spindle is attached to the egg cortex by one pole during anaphase to allow selective disposal of half the chromosomes in a polar body. In *Caenorhabditis elegans*, this anaphase spindle position is achieved sequentially through kinesin-1–dependent early translocation followed by anaphase-promoting complex (APC)-dependent spindle rotation. Partial depletion of cytoplasmic dynein heavy chain by RNA interference blocked spindle rotation without affecting early translocation. Dynein depletion also blocked the APC-dependent late translocation that occurs in kinesin-1–depleted embryos. Time-lapse imaging of green fluorescent protein-tagged dynein heavy chain as well as immunofluorescence with dynein-specific antibodies revealed that dynein starts to accumulate at spindle poles just before the initiation of rotation or late translocation. Accumulation of dynein at poles was kinesin-1 independent and APC dependent, just like dynein driven spindle movements. This represents a case of kinesin-1/dynein coordination in which these two motors of opposite polarity act sequentially and independently on a cargo to move it in the same direction.

INTRODUCTION

Kinesin-1, a plus-end–directed microtubule motor, and cytoplasmic dynein, a minus-end–directed motor, frequently act together in the bidirectional transport of cellular cargoes. In axons, microtubules are arranged in a parallel orientation with plus ends oriented toward the nerve terminal and minus ends oriented toward the cell body (Baas *et al*., 1988). Mitochondria move bidirectionally on these highly oriented microtubule tracks, with kinesin-1 transporting mitochondria toward the nerve terminal and cytoplasmic dynein moving mitochondria toward the cell body (Pilling *et al*., 2006). *Drosophila* embryos have radial microtubule arrays with minus ends at the cortex and plus ends in the interior of the embryo. Lipid droplets exhibit bidirectional transport on these microtubules with kinesin-1 moving droplets toward plus ends in the interior (Shubeita *et al*., 2008) and cytoplasmic dynein moving droplets toward minus ends at the cortex (Gross *et al*., 2000). Drosophila S2 cells extend long processes containing parallel microtubule bundles with minus ends oriented toward the centrosome and plus ends oriented toward the periphery. Peroxisomes move bidirectionally on these microtubule bundles with kinesin-1 moving peroxisomes toward the distal ends of the processes and cytoplasmic dynein moving peroxisomes toward the centrosome (Kural *et al*., 2005). In each of these cases, kinesin-1 and cytoplasmic dynein transport cargoes toward different regions of the cell because microtubules have a parallel or radial organization. In addition, transport of cargo switches frequently between kinesin-1–mediated and dynein-mediated transport, even during net movement in one direction (Kural *et al*., 2005).

Here, we report that kinesin-1 and cytoplasmic dynein act sequentially to move the meiotic spindle in the same direction toward the cortex of the *Caenorhabditis elegans* meiotic embryo. This is a fundamentally different type of coordination between kinesin-1 and cytoplasmic dynein and requires that either the polarity of microtubules in the cell switches between the early action of kinesin-1 and the late action of dynein or that kinesin-1 and dynein can act specifically on different classes of microtubules present in the cell.

The *C. elegans* meiotic spindle initially assembles 4 μm away from the cell cortex and moves toward the cortex in a sideways orientation at 1 μm/min and assumes an orientation parallel to the cortex (Yang *et al*., 2003, 2005). The metaphase spindle maintains a constant pole–pole length and parallel orientation at the cortex for 6 min before initiating an ordered sequence of events that all depend on the anaphase-promoting complex (APC). On APC activation, the spindle begins to shorten in the pole–pole axis, it then rotates to a perpendicular orientation, and anaphase chromosome segregation initiates as the spindle continues to shorten. After reaching a minimum length, the spindle then elongates in an anaphase B-like process as cytokinesis occurs. These events repeat in meiosis II (Yang *et al*., 2003, 2005). The net result of these movements is the expulsion of half the homologous chromosomes in the first polar body and half the remaining sister chromatids in the second polar body, while maintaining the volume of the egg.

We found previously that the early translocation to the cortex is independent of the APC but dependent on microtubules, kinesin-1 heavy chain, kinesin light chain, and a light chain-binding protein, KCA-1. These results indicated that a complex of kinesin-1 and KCA-1 transport the spindle toward the cortex on microtubules. After initiation of APC-

This article was published online ahead of print in *MBC in Press* (http://www.molbiolcell.org/cgi/doi/10.1091/mbc.E08–12–1253) on April 8, 2009.

Address correspondence to: Francis J. McNally (fjmcnally@ucdavis.edu).

Abbreviations used: APC, anaphase-promoting complex.

dependent spindle shortening, meiotic spindles in kinesin-depleted embryos suddenly move to the cortex by a ''late'' translocation mechanism that is kinesin independent but APC dependent (Yang *et al*., 2005). We hypothesized that late translocation in kinesin-1–depleted embryos is driven by the same motor that drives meiotic spindle rotation in a wild-type embryo. This hypothesis was supported by three observations. Wild-type rotation and late translocation are both APC dependent, they occur at the same time during the spindle shortening cycle, and they both involve pole-first movement toward the cortex (Yang *et al*., 2005). Because cytoplasmic dynein, acting through a cortical pulling mechanism, is responsible for pole-first spindle movements in other organisms (Sheeman *et al*., 2003), we tested whether cytoplasmic dynein is the motor driving APC-dependent meiotic spindle rotation and late translocation.

MATERIALS AND METHODS

C. elegans Strains

Strains were cultured according to standard procedures (Brenner, 1974). In this study, wild type indicates the integrated green fluorescent protein (GFP): tubulin strain AZ244 (Praitis *et al*., 2001), which was derived from N2. *unc-116(rh24sb79)* is a partial loss-of-function mutation that has some unc-116(+) activity and the strain has integrated GFP-tubulin (Yang *et al*., 2005). The strain in Figures 3, 4, and 5 is EU1561, which has integrated GFP-dynein (DHC-1) and mCherry:histone H2B transgenes (Gassmann *et al*., 2008; McNally *et al*., 2006). Strains in Supplemental Figure 2 are as follows: WH258 with integrated GFP:DNC-2 (Zhang *et al*., 2008), WH257 with integrated GFP:DNC-1 (Zhang *et al*., 2008), and EU1426 with integrated GFP:DYRB-1 (O'Rourke *et al*., 2007). AZ244 was maintained at 20°C and all other strains were maintained at 25°C to prevent germline silencing. All strains were shifted to 25°C for 24 h before filming.

In Utero Live Imaging

Adult hermaphrodites were anesthetized with tricaine/tetramisole as described previously (Kirby *et al*., 1990; McCarter *et al*., 1999) and gently mounted between a coverslip and a thin agarose pad on a slide. Imaging was carried out, as described previously (Yang *et al*., 2003), with a microscope (Microphot SA; Nikon, Tokyo, Japan) equipped with a 60× PlanApo 1.4 objective and a charge-coupled device ([CCD], Qimaging Retiga Ex*i* Fast 1394 camera). Excitation light from an HBO100 light source was attenuated with a heat and UV reflecting ''hot mirror'' (Chroma Technology, Brattleboro, VT) and a 25% transmission neutral density filter. A GFP long pass filter set (Omega Optical, Brattleboro, VT) was used. Excitation light was shuttered with a Sutter shutter controlled by a Sutter Lambda 10-3 controller and IVision software (BioVision Technologies, Exton, PA). Stage temperature was 22–24°C. Exposures of 0.2–0.6 s were captured at 3-, 5-, or 15-s intervals for 20–40 min. Every embryo was followed through extrusion of the second polar body to ensure that meiosis was not arrested due to photodamage. All quantitative analysis was carried out with IVision software. Exit from the spermatheca was used as T = 0 for timing because this is technically more feasible than starting time-lapse sequences at nuclear envelope breakdown. Although the amount of time that an embryo resides in the spermatheca is variable (McCarter *et al*., 1999), there is relatively uniform timing between exit of the spermatheca and many meiotic events including completion of spindle rotation (McNally and McNally,2005), spindle contact with the cortex (Yang *et al*., 2005), and APC activation/spindle shortening (Yang *et al*., 2005). Thus, using exit from the spermatheca as a start point allows comparison of the relative timing of meiotic events between genotypes.

RNA Interference (RNAi)

All of the RNAi experiments performed in this study were carried out by feeding bacteria (HT115) induced to express double-stranded RNA corresponding to each gene as described by Timmons *et al*. (2001) and by Kamath *et al*. (2000). L4 hermaphrodites were transferred to RNAi plates and allowed to feed on the RNAi bacterial lawn for 16–36 h. HT115 harboring the L4440 vector only was used as the bacterial lawn for the control experiments shown in Figures 1A and 2A, Table 1, and Supplemental Table 1. The following clones from the genomic RNAi feeding library (MRC Gene Services, Source BioScience, Cambridge, United Kingdom; Kamath *et al*., 2000) were used: *dhc-1* clone I-1P04, *kca-1* clone I-2109, and *mat-1* clone I-2C18. One hundred percent embryonic lethality was observed after 24 h of feeding for *dhc-1(RNAi)* and *mat-1(RNAi)*. For imaging, 24-h feeding was used for *dhc-1(RNAi)* in the AZ244 strain, and 16-h feeding was used for *dhc-1(RNAi)* in the *unc-116(rh24sb79)* strain because it seemed to be more susceptible to severe *dhc-1(RNAi)* phenotypes. Twenty-four-hour feeding was used for *mat-1(RNAi)* in the EU1561 strain, and 36 h feeding was used for *kca-1(RNAi)* in the EU1561 strain. The phenotype observed in *kca-1(RNAi)* was similar to that observed for *unc-116(rh24sb79)* worms. All RNAi feeding experiments were carried out at 25°C.

Measurements and Quantification

All measurements of spindle length, distance from the cortex (Supplemental Table 1), and linear velocities during spindle rotation (Table 1) were made from single focal plane time-lapse sequences by using IVision software. Measurements were made only from image sequences where the spindle orientation could be unambiguously determined from the direction of microtubule bundles within the spindle and both spindle poles were in sharp focus, indicating that the spindle was parallel to the plane of focus.

In Supplemental Table 1, spindle length was measured as the distance along the pole-to-pole axis. The pole-to-pole axis was determined from thick fluorescent bars of GFP:tubulin (TUB) that represent dense bundles of microtubules extending along the pole-to-pole axis. Spindle length was measured as the length of the longest bar of GFP:TUB fluorescence in each frame of a time-lapse sequence. To determine the accuracy of these measurements, 10 measurements of spindle length were made for each spindle. The SD of these measurements was 0.2 μm. Distance between the spindle and the cortex was measured as the shortest distance between the edge of the spindle and the cortex.

To measure linear velocity of a spindle pole during spindle rotation (Table 1), a straight line was drawn between the spindle pole that moves toward the cortex and the point on the cortex where the pole made contact after rotation. The point chosen as the spindle pole was the end of the fluorescent bar of GFP:TUB that extends along the pole-to-pole axis. Using the IVision segmentation tool, a mark was drawn where the spindle pole contacted the cortex after rotation. In each image acquired before rotation, a line was drawn between the current position of the spindle pole and the fixed mark on the cortex. The length of this line was measured for each frame during spindle rotation, and Excel (Microsoft, Redmond, WA) was used to plot the distance over time. The slope of the line of best fit was used to infer average linear velocity. This method does not require locating the exact edge of the cortex in every frame but instead relies only on determining the position of the spindle pole at the end of rotation. To determine the accuracy of these measurements, 10 measurements were made for each time-lapse sequence. The SD among these measurements was 0.003 μm/s. This method is subject to errors caused by slight movements of the worm during time-lapse imaging. These errors are included in the standard deviations between time-lapse sequences which are shown in Table 1. The same method was used to measure the velocity of late-translocation in *unc-116* embryos.

GFP:DHC-1 fluorescence intensity (Figures 3 and 4) was measured along a line drawn down the length of the pole-to-pole axis. The length and orientation of the spindle was determined from DHC-1 localization on the poles and from chromosome positioning (mCherry:Histone). Using Excel, pixel intensity was plotted against spindle length (length along the drawn line). Background fluorescence, determined from the cytoplasm near the spindle, was subtracted from each spindle measurement. Fluorescence intensity was determined for each frame of a time-lapse sequence starting at 2 min before the start of rotation through 2 min after the start of rotation.

Antibodies and Immunostaining

Immunostaining was performed using standard freeze-fracture methods followed by −20°C methanol fixation as described previously (Tsou *et al*., 2002; DeBella *et al*., 2006). Primary antibodies were diluted in phosphate-buffered saline containing 0.05% Tween 20 (PBST) in the following ratios: anti-DHC-1 antibody (Gönczy *et al*., 1999), 1:200; anti-tubulin DM1α (Sigma-Aldrich, St. Louis, MO), 1:200; anti-DNC-1 (Skop and White, 1998), 1:200; and anti-LIN-5 (Park and Rose, 2008), 1:50. All secondary antibodies (Invitrogen, Carlsbad, CA) were diluted 1:200 in PBST. 4,6-Diamidino-2-phenylindole (DAPI) staining was used to visualize DNA and specimens were mounted with VECTASHIELD (Vector Laboratories, Burlingame, CA). Stained embryos were imaged using a 60× objective on a DeltaVision-real-time deconvolution microscope (Applied Precision, Issaquah, WA) equipped with a Photometrics CoolSNAP HQ CCD camera (Roper Scientific, Trenton, NJ). Images were deconvolved using softWoRx Explorer Suite software (Applied Precision).

RESULTS

In dhc-1 (RNAi) Embryos, the Meiotic Spindle Does Not Rotate Perpendicular to the Oocyte Cortex

To determine whether cytoplasmic DHC-1 is required for meiotic spindle positioning, we recorded time-lapse sequences of meiotic spindle movements in worms expressing GFP-tubulin and depleted of DHC-1 by RNAi. Because complete loss of cytoplasmic dynein results in disorganized meiotic spindles and sterile adult worms (Gönczy *et al*., 1999;

Yang *et al*., 2005), we analyzed the effect of partial depletion of DHC-1 by subjecting worms to RNAi by feeding for 24 h. At this time, bipolar spindle formation, metaphase spindle length, early translocation, spindle shortening, and cell cycle timing seemed normal (Supplemental Table 1). In 100% of wild-type worms (Figure 1A), spindle rotation initiated 1.8 ± 0.2 min (average of meiosis I and II, n = 19) after the initiation of spindle shortening (Supplemental Table 1), and one spindle pole moved toward its final position on the cortex along a linear track (Figure 1C) at a velocity of 0.05 ± 0.01 μm/s (Table 1). In *dhc-1(RNAi)* worms (Figure 1B), spindle shortening initiated at a similar time as wild type (5.1 ± 0.4 min after exit from the spermatheca for meiosis I and 6.0 ± 0.3 min after first polar body extrusion for meiosis II; Supplemental Table 1), but no rotation was observed in 79% of meiosis I events and 87% of meiosis II events (Table 1). In these embryos, the meiotic spindle remained parallel at the cortex after initial spindle shortening and stayed parallel at the cortex through the completion of anaphase. Failure to rotate the meiotic spindle to a perpendicular orientation at the oocyte cortex resulted in abnormal polar body extrusion (Table 1; Supplemental Figure 1), and, in some cases, polyploid embryos (Supplemental Figure 1). In the minority of *dhc-1 (RNAi)* embryos where the meiotic spindle did rotate, rotation occurred at a slower velocity than wild type (Table 1), suggesting that there was incomplete knockdown of dynein activity. These observations suggest that cytoplasmic dynein is a microtubule motor required for meiotic spindle rotation and that the mechanism of spindle rotation is distinct from the mechanism of early spindle translocation, as dynein does not seem to be required to position the metaphase spindle in a parallel orientation at the oocyte cortex.

UNC-116 and DHC-1 Act Independently to Position the Meiotic Spindle

Early meiotic spindle translocation to the parallel orientation at the oocyte cortex is dependent on the plus-end–directed microtubule motor kinesin-1, UNC-116. In UNC-116–depleted embryos, the meiotic spindle fails to translocate to the oocyte cortex early in meiosis, but moves to the cortex by a ''late'' translocation mechanism that we previously hypothesized was due to the same mechanism that drives wild-type rotation (Yang *et al*., 2005). To determine whether DHC-1 is required for UNC-116–independent late translocation, we analyzed meiotic spindle movements in *unc-116(rh24sb79)* mutant embryos that were also depleted of DHC-1 by RNAi.

In *unc-116* single mutant embryos, early spindle translocation failed and late meiotic spindle translocation initiated 1.7 min (average of meiosis I and II) after initiation of spindle shortening (Figure 2A and Supplemental Table 1). Late translocation proceeded on a linear track (Figure 2C) at a velocity of 0.06 μm/s (Table 1), similar to the velocity of wild-type rotation. In *unc-116;dhc-1(RNAi)* double mutant embryos, both early translocation and late translocation failed (Figure 2B). In all *unc-116* mutant embryos where *dhc-1* activity was efficiently reduced, the meiotic spindle remained several micrometers from the cortex and did not undergo any directed movement toward the cortex before or after APC activation. In these embryos, the meiotic spindle completed anaphase far from the cortex and polar body extrusion was severely abnormal (Table 1), with multiple ectopic furrows forming (Supplemental Figure 1). In 5/10 *unc-116;dhc-1 (RNAi)* double mutant embryos, extrusion of the first polar body completely failed and two meiosis II spindles assembled (Figure 2B). In embryos with two meiosis II spindles, the two spindles sometimes completed an-

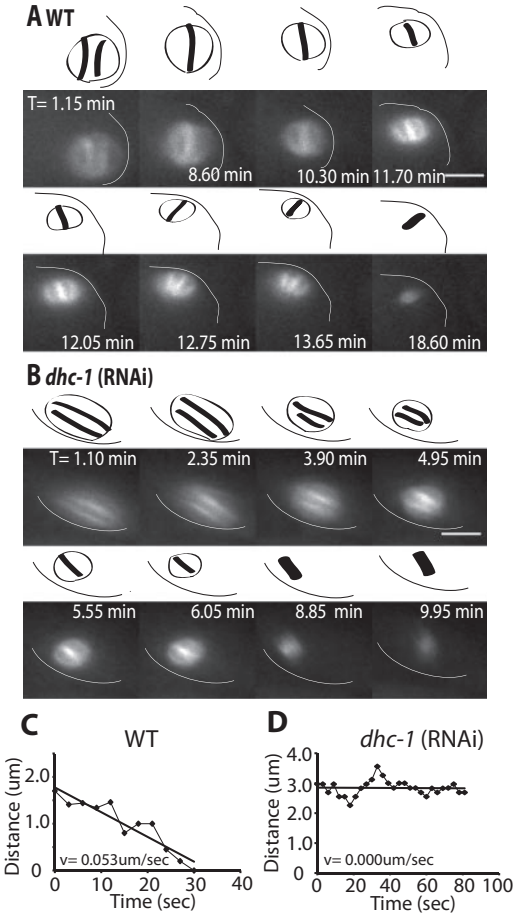

Figure 1. *dhc-1(RNAi)* spindles remain parallel at the cortex after APC activation. Images of GFP-tubulin fluorescence within a meiotic embryo are shown from representative time-lapse sequences from a wild-type worm (A) and a *dhc-1(RNAi)* worm. (B) Zero minutes (0 min) corresponds to exit of the embryo from the spermatheca. The cell cortex was highlighted in each image for clarity. Drawings corresponding to each image are included for clarity to show spindle orientation and length. Spindle orientation was determined from dense bundles of microtubules that extend along the pole-to-pole axis. (A) The wild-type meiosis I spindle translocated to the cortex within 1 min of exiting the spermatheca and adopted an orientation parallel to the cortex. The spindle began to shorten between 8.6 and 10.3 min, indicating activation of the APC. During shortening, the spindle rotated between 11.7 and 12.7 min, ending in a position perpendicular to the cortex. (B) In the *dhc-1(RNAi)* embryo, the meiotic spindle also translocated to the cortex within 1 min of exit from the spermatheca and began to shorten at 4 min. During spindle shortening, the spindle remained parallel at the cortex and did not undergo rotation. The spindle completed anaphase while remaining parallel to the cortex. Corresponding Supplemental Videos 1 and 2 can be found in the online supplemental material. (C and D) Representative graphs of spindle movement over time after initiation of spindle shortening corresponding to the time-lapse sequences in A and B, respectively. In wild type (C), distance was measured between the current position of the pole that is proximal to the cortex after rotation and the point on the cortex where that spindle pole made contact at the end of rotation. The straight line represents the line of best fit for the raw measurements taken (◆). This meiotic spindle moved to the cortex on a linear track with a velocity of 0.053 μm/s. (D) In *dhc-1(RNAi)* embryos, distance was measured from one spindle pole to an arbitrary point at the cortex during the period of spindle shortening when rotation would occur in a wild-type embryo. The spindle made no directed movement toward the cortex resulting in a net velocity of 0 μm/s. Bars, 5 μm.

Table 1. Spindle rotation and polar body extrusion

	Wild type	*unc-116*	*dhc-1(RNAi)*	*unc-116; dhc-1(RNAi)*
Rotation (MI)				
Rotation	14	14	5	1
Linear velocity[a] (μm/s)	0.049 ± 0.008 (n = 8)	0.053 ± 0.004 (n = 13)	0.021 ± 0.002[b] (n = 3)	0.055[b] (n = 1)
No rotation	0	0	19	12
Total	14	14	24	13
Rotation (MII)				
Rotation	8	8	2	3
Linear velocity (μm/s)	0.052 ± 0.01 (n = 4)	0.065 ± 0.005 (n = 5)	0.046[b] (n = 1)	0.074 ± 0.011[b] (n = 3)
No rotation	0	0	13	7
Total	8	8	15	10
Polar body extrusion (MI)				
Normal	11	13	3	1
Abnormal	1	0	14	12
Total	12	13	17	13
Polar body extrusion (MII)				
Normal	5	8	1	0
Abnormal	1	0	14	10
Total	6	8	15	10
Two MII spindles assemble	0 (n = 8)	0 (n = 8)	3 (n = 15)	5 (n = 10)

Numbers indicate number of spindles for each genotype from time-lapse sequences of meiosis where parameters were measurable. MI, meiosis I; MII, meiosis II.

[a] Linear velocity indicates the velocity of one spindle pole moving toward a fixed point on the cortex during spindle rotation.

[b] Linear velocities taken from films where spindle did rotate after dhc-1 RNAi, velocities of films with no rotation are not included.

aphase separately (Supplemental Figure 1) and sometimes merged into a single spindle before completing anaphase. These results indicate that kinesin-1 and cytoplasmic dynein act sequentially and independently to position the meiotic spindle.

DHC-1 Is Localized Uniformly on Metaphase Meiotic Spindles and Relocalizes to Spindle Poles Immediately before the Initiation of Rotation and Late Translocation

Because spindle shortening requires the APC (Yang *et al*., 2003, 2005), initiation of spindle shortening is a visual indication of APC activation. Because dynein-mediated rotation and late translocation start suddenly at a discrete time after initiation of shortening (Supplemental Table 1), we looked for changes in dynein localization that might occur at this time in the cell cycle and which might be mediated by the APC.

To monitor dynamic changes in the localization of cytoplasmic dynein, we recorded time-lapse sequences of meiotic spindles by using a strain expressing GFP:DHC-1 and mCherry:Histone (Gassmann *et al*., 2008). During eight of eight time-lapse sequences of wild-type meiosis, GFP:DHC-1 was uniformly localized throughout the meiotic spindle before APC activation (Figure 3A). Within 45–30 s before spindle rotation, GFP:DHC-1 began to accumulate at both spindle poles and continued to accumulate at the meiotic spindle poles through rotation. After rotation, GFP:DHC-1 stayed on the meiotic spindle poles but did not accumulate further. In some cases, DHC-1 accumulated slightly more on one pole versus the other (Figure 3B), but there was no consistent trend of which pole was brighter between the proximal pole (near the cortex) and distal pole, unlike dynein in *Saccharomyces cerevisiae*, which has been reported to accumulate more on the pole moving toward the bud cortex (Grava *et al*., 2006). Because of limitations to our imaging, we cannot exclude the possibility that dynein accumulates asymmetrically on the pole that moves toward the cortex. Nonetheless, DHC-1 accumulated on meiotic spindle poles during rotation in every embryo observed. The accumulation of dynein at spindle poles during spindle shortening is not explained simply by changes in spindle structure. Although the fluorescence intensity of GFP-tubulin increases during the first phase of spindle shortening (McNally *et al*., 2006), this increase occurs uniformly throughout the spindle and thus does not explain the specific increase in dynein concentration at poles. It is also unlikely that dynein's accumulation at poles is driving spindle shortening because shortening occurs normally in *dhc-1(RNAi)* embryos (Figure 1B and Supplemental Table 1) even when metaphase spindle structure is severely disrupted (Yang *et al*., 2005).

To confirm the localization pattern of GFP:DHC-1, we determined the localization of endogenous dynein heavy chain by staining fixed, meiotic embryos with an anti-DHC-1 antibody (Gönczy *et al*., 1999). Endogenous DHC-1 was localized uniformly on metaphase meiotic spindles and concentrated at poles of rotated meiotic spindles (Figure 3C). Furthermore, known cytoplasmic dynein regulators, including dynactin (n = 5/5), dynamitin (n = 10/10), dynein roadblock (n = 9/9), and LIN-5 all had similar localization patterns during meiotic spindle positioning (Supplemental Figure 2). These data demonstrate that DHC-1 relocalizes to spindle poles at the same time that dynein-dependent movement of the spindle pole to the cortex is occurring.

To test whether the late spindle translocation that occurs in kinesin-1–depleted embryos is indeed due to the same dynein-dependent mechanism as wild-type rotation, the localization of GFP:DHC-1 was monitored in *kca-1(RNAi)* embryos. KCA-1 binds to kinesin-1 through its light chain and is required for early spindle translocation (Yang *et al*., 2005). In *kca-1(RNAi)* embryos (n = 4/4), early meiotic spindle translocation failed, however, GFP:DHC-1 relocalized to spindle poles with kinetics identical to that observed in wild type (Figure 4A). GFP:DHC-1 was localized uniformly on

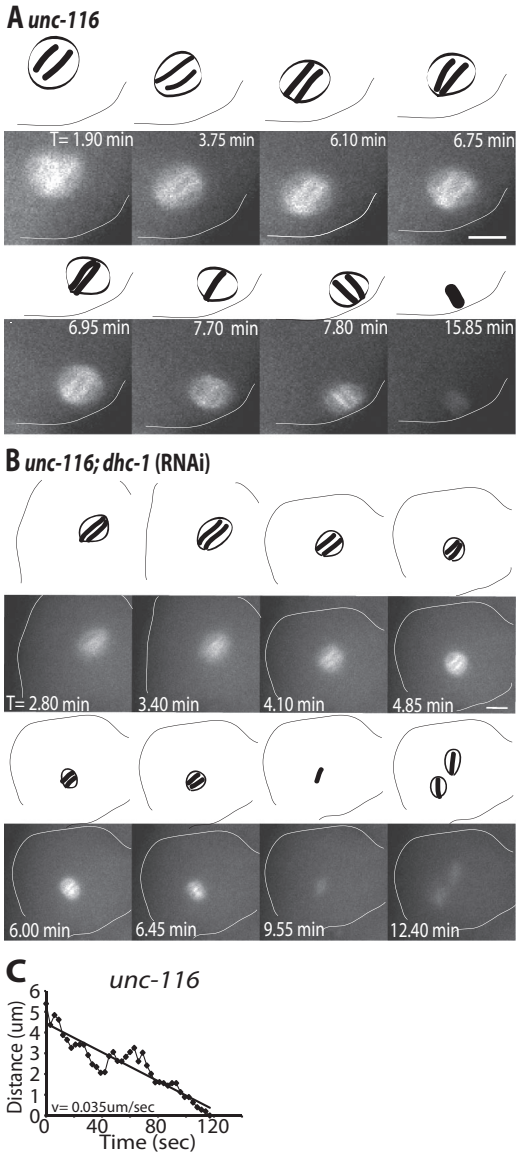

Figure 2. *unc-116;dhc-1(RNAi)* spindles fail to undergo directed movement toward the cortex. Images of GFP-tubulin fluorescence within a meiotic embryo are shown from representative time-lapse sequences from an *unc-116* worm (A) and a *unc-116;dhc-1(RNAi)* worm (B). Zero minutes (0 min) corresponds to exit of the embryo from the spermatheca. The cell cortex was highlighted in each image for clarity. Drawings corresponding to each image are included for clarity to show spindle orientation and length. Spindle orientation was determined from dense bundles of microtubules that extend along the pole-to-pole axis. (A) The *unc-116* spindle failed to translocate early to the cortex and remained stationary at a position several micrometers from the cortex from 0 to 6.70 min. Spindle shortening initiated just before the start of late translocation to the cortex (6.75–7.80 min). The spindle undergoes late, pole-leading translocation to the cortex ending perpendicular to the cortex (7.80 min). (B) In the *unc-116;dhc-1(RNAi)* embryo, the spindle remained away from the cortex throughout meiosis and failed to undergo directed movement toward the cortex. The spindle completed meiosis I away from the cortex and two meiosis II spindles assembled (T = 12.4 min). Corresponding Supplemental Videos 3 and 4 can be found in the online supplemental material. (C) Representative graph of *unc-116* spindle movement over time after spindle shortening. Distance was measured as described for wild type in Figure 1 (C). The *unc-116* spindle translocated to the cortex following a linear track with a velocity of 0.035 μm/s. Bars, 5 μm.

the metaphase meiotic spindle and then began to accumulate on spindle poles 30–45 s before late translocation and continued to accumulate at spindle poles through late translocation. As in wild-type embryos, GFP:DHC-1 accumulated symmetrically on both spindle poles in *kca-1(RNAi)* embryos (Figure 4B). The localization pattern of dynein regulators was also unaffected in *kca-1(RNAi)* embryos (Supplemental Figure 3). These results support the model that wild-type rotation and late translocation are driven by the same dynein-dependent mechanism.

Redistribution of Cytoplasmic Dynein to Spindle Poles Requires the APC

Spindle rotation and late translocation both require the APC and occur at the same time as other APC-dependent events, such as spindle shortening (Yang *et al*., 2005). Because rotation and late translocation are driven by cytoplasmic dynein, we hypothesized that the APC may activate cytoplasmic dynein at the appropriate time during the cell cycle. To test this hypothesis, we analyzed GFP:DHC-1 localization in embryos depleted of MAT-1, which encodes the CDC27/APC3 subunit of the APC and is required for the metaphase to anaphase transition in meiosis I (Golden *et al*., 2000, Shakes *et al*., 2003). In GFP:DHC-1;*mat-1(RNAi)* embryos (n = 6/6), the meiotic spindle arrested in metaphase I and did not undergo spindle shortening or spindle rotation (Figure 5). In the absence of the APC, GFP:DHC-1 localized uniformly on the meiotic spindle but did not accumulate at spindle poles in embryos that were filmed for >40 min after fertilization. This result indicates that the APC is required for DHC-1 accumulation on meiotic spindle poles and suggests that the APC may initiate spindle rotation by activating cytoplasmic dynein.

Microtubules Extend between the Meiotic Spindle and the Cortex

To help distinguish between possible mechanisms of dynein-mediated spindle movements, we looked for microtubule and dynein heavy chain interactions in the area between the meiotic spindle and the cortex. Anti-tubulin immunofluorescence revealed that numerous microtubules fill the entire volume of the meiotic embryo and that these microtubules contact both the spindle and the cortex (Figure 6, A–C). If any astral microtubules extend in a straight line between one spindle pole and the cortex, they are obscured in most images by numerous cytoplasmic microtubules that have no apparent, ordered orientation relative to the spindle or cortex.

To determine whether cytoplasmic dynein might specifically interact with a subset of these microtubules, we carefully analyzed time-lapse sequences of GFP:DHC-1 in wild-type embryos specifically during spindle rotation. In rare cases, a linear track of GFP:DHC-1 extended between the spindle and the cortex before or during rotation (Supplemental Figure 4, A and B). In some cases, the spindle clearly rotated toward a cortical patch of GFP:DHC-1 (Supplemental Figure 4, B and C). The low contrast between cytoplasmic GFP:DHC-1 and cortical GFP:DHC-1 in most images made it impossible to unambiguously determine whether GFP:DHC-1 was distributed evenly around the entire cortex or whether it was specifically concentrated on the cortex near the spindle. In addition, in some fixed embryos stained with anti-DHC-1, dynein localized to cortical areas proximal to the spindle (Supplemental Figure 4D). Occurrence of GFP:DHC-1 on microtubules extending from the spindle or in patches on the cortex was rare and further analysis of this localization is limited by our im-

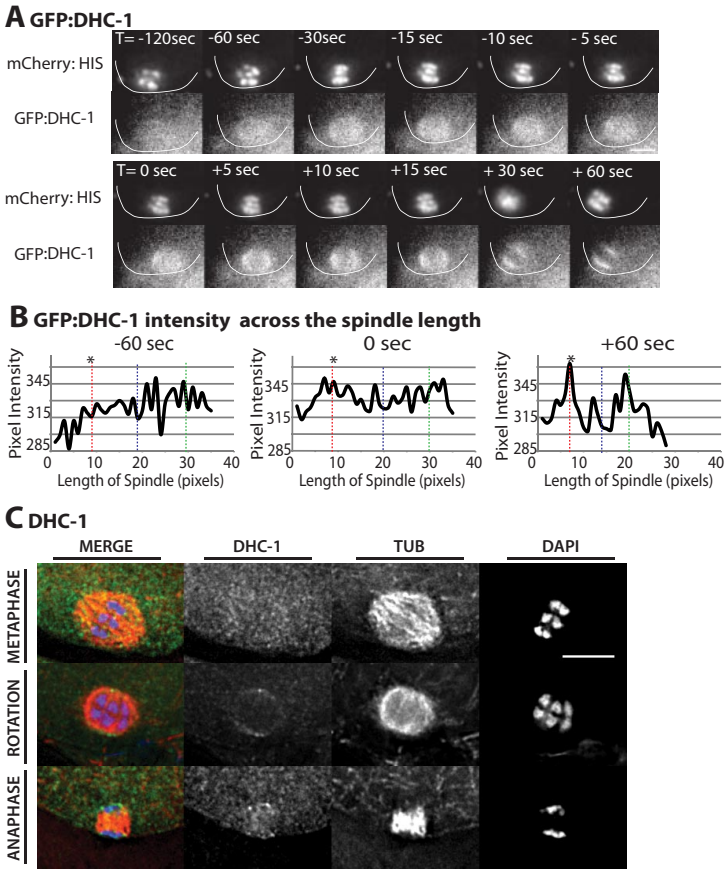

Figure 3. DHC-1 accumulates on meiotic spindle poles during rotation. (A) Images of mCherry-histone (top row) and GFP: DHC-1 (bottom row) within a wild-type meiotic embryo are shown from a representative time-lapse sequence. The cortex has been highlighted in each image for clarity. 0 s is the start of rotation. GFP: DHC-1 was faintly localized across the meiotic spindle before spindle shortening (T = −120 s). 45–30 s before the start of spindle rotation, DHC-1:GFP began to accumulate on meiotic spindle poles and remained on meiotic spindle poles after spindle rotation (T = +60 s). (B) Graphs of GFP:DHC-1 pixel intensity. Intensity was measured from line-scans down the pole–pole axis of the meiotic spindle for each frame of the representative wild-type time-lapse sequence in A. Only three time points are shown. The vertical dashed lines indicate the positions of the middle of the spindle (blue) and the two spindle poles (red and green). The asterisk (*) indicates which pole contacted the cortex after rotation. (C) Immunostaining of anti-DHC-1 in fixed wild-type embryos, costained with anti-tubulin (TUB) and DAPI to visualize the chromosomes. The top row shows a metaphase spindle with DHC-1 faintly localized throughout the spindle. The middle row shows a rotated spindle before chromosome segregation with anti-DHC-1 localized to the spindle poles. The bottom row is an anaphase spindle with DHC-1 localized to the spindle poles. Bars, 5 μm.

aging capabilities. Although not conclusive, these results are consistent with the hypothesis that cortical dynein drives spindle rotation by pulling on astral microtubules extending from the spindle.

DISCUSSION

In well characterized systems such as axons, *Drosophila* S2 cells, and the *Drosophila* embryo, microtubules have a parallel or radial organization and kinesin-1 and cytoplasmic dynein move cargo to opposite regions of the cell. In the *C. elegans* meiotic embryo, kinesin-1 drives early translocation toward the cortex (Yang *et al*., 2005), and cytoplasmic dynein moves one spindle pole toward the cortex during rotation and late translocation (van der Voet *et al*., 2009; this study). This observation raises two fundamental questions that have broad relevance to intracellular transport: 1) How do two motors with opposite polarity move the same cargo in the same direction?, and 2) How is cytoplasmic dynein activated at a precise point in the cell cycle?

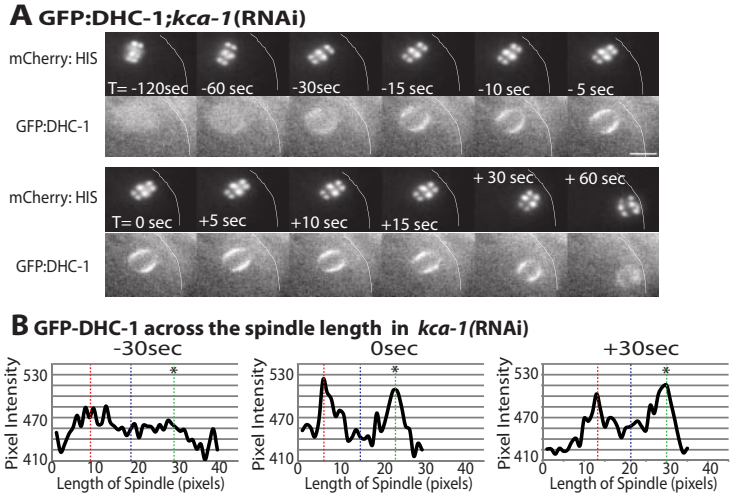

Figure 4. In the absence of KCA-1, DHC-1 accumulates on meiotic spindle poles during late spindle translocation. (A) Images of mCherry:histone (top row) and GFP: DHC-1 (bottom row) within a meiotic embryo are shown from a representative time-lapse sequence of a *kca-1(RNAi)* worm. The cortex has been highlighted in each image for clarity. 0 s is the start of late translocation. GFP:DHC-1 faintly localized across the meiotic spindle before spindle shortening (T = −120 s). Forty-five to 30 s before the start of late spindle translocation, GFP:DHC-1 began to accumulate on meiotic spindle poles and remained on meiotic spindle poles after late translocation (T = +60 s). (B) Graphs of GFP:DHC-1 pixel intensity. Intensity was measured from line-scans down the pole-pole axis of the meiotic spindle for each frame of the representative *kca-1(RNAi)* time-lapse sequence in A. Only three time points are shown. The vertical dashed lines indicate the positions of the middle of the spindle (blue) and the two spindle poles (red and green). The asterisk (*) indicates which pole contacts the cortex after rotation. Bar, 5 μm.

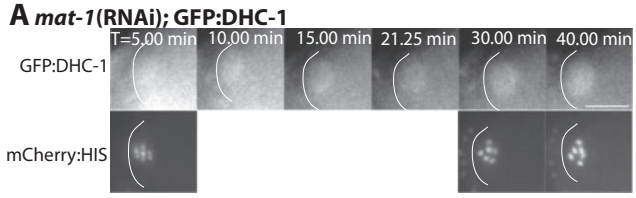

Figure 5. mat-1(RNAi) blocks accumulation of GFP:DHC-1 on meiotic spindle poles. (A) Images of GFP:DHC-1 (top row) and mCherry:histone (bottom row) within a meiotic embryo are shown from a representative time-lapse sequence of a *mat-1(RNAi)* worm. Zero minutes (0 min) corresponds to exit of the embryo from the spermatheca. The cell cortex was highlighted in each image for clarity. GFP:DHC-1 localizes faintly to the metaphase meiotic spindle (T = 5–10 min). GFP:DHC-1 remains localized uniformly to the arrested metaphase spindle for >40 min and no accumulation of GFP:DHC-1 on the meiotic spindle poles is observed. Bar, 10 μm.

Models Explaining the Polarity Paradox

In *S. cerevisiae*, the coordinated activities of the plus-end–directed motor Kip3 and cytoplasmic dynein move the mitotic spindle toward the bud cortex. However, the motor activity of kip3 is used only to target kip3 to the plus end of an astral microtubule. When the plus end contacts the cortex, kip3 docks on the cortex and the depolymerase activity of kip3 then generates a cortical pulling force (Gupta *et al*., 2006). In contrast, dynein generates a pulling force in the same direction through its minus-end–directed motor activity (Sheeman *et al*., 2003). This type of mechanism is unlikely in the *C. elegans* meiotic embryo because extensive biochemical characterization of kinesin-1 has never uncovered a depolymerase activity in kinesin-1, and kinesin-1–driven spindle translocation occurs in a sideways orientation.

A more likely model explaining the polarity paradox suggests that, in the apparently randomly oriented cytoplasmic microtubule array, more microtubule plus ends are pointed toward the cortex than are pointed toward the interior of the embryo (Figure 7). In this scenario, kinesin-1 bound to the spindle through KCA-1 would pull the spindle in all directions but with a net pulling force toward the cortex. On APC activation, inhibitors of dynein motility and/or astral microtubule growth would be proteolyzed (Figure 7A). Dynein would then be transported on the growing plus ends of astral microtubules and activated upon docking at a cortical site, where it would generate a cortical pulling force acting on spindle poles (Sheeman *et al*., 2003). In this model, the cargo-binding region of dynein is not associated with the spindle so that it does not generate force on the cytoplasmic microtubule array. Elongation of astral microtubules specifically during mitotic anaphase is seen in many organisms, including *C. elegans* (Gönczy *et al*., 2001). It is generally thought that acentriolar spindles do not extend astral microtubules; however, the acentriolar spindles of parthenogenetically activated mammalian oocytes extend long astral microtubules specifically at anaphase (Navara *et al*., 1994).

In an alternative model, cytoplasmic microtubules have a majority of plus ends pointed toward the cortex before APC activation and a majority of minus ends pointed toward the cortex after APC activation (Figure 7B). This model suggests that the dynein at spindle poles is attached to the spindle through the cargo-binding domain to allow the motor domains to interact with the cytoplasmic microtubules after APC activation. The reversal of microtubule polarity could be driven by an APC-activated cortical nucleator. A model in which the majority of microtubules in a seemingly random microtubule array are oriented in a specific direction has been suggested in *Drosophila* oocytes. In these cells, cytoplasmic microtubules are thought to have a majority of minus ends pointed toward the cortex because γ-tubulin, a minus-end capping protein, is enriched at the cortex and because kinesin-1 cargoes accumulate at the cortex when kinesin-1 is depleted (Cha *et al*., 2002). Similar experiments in *C. elegans* indicate that γ-tubulin is enriched on the nuclear envelope just before meiotic maturation (McNally *et al*., 2006) and kinesin cargo (the spindle) accumulates away from the cortex when kinesin-1 is depleted. These results support the idea that, before APC activation, there is a net polarity with plus ends pointed toward the cortex. γ-Tubulin was not observed relocalizing to the cortex at anaphase, so there is currently no support for the idea of a polarity reversal of the cytoplasmic microtubule array during the cell cycle.

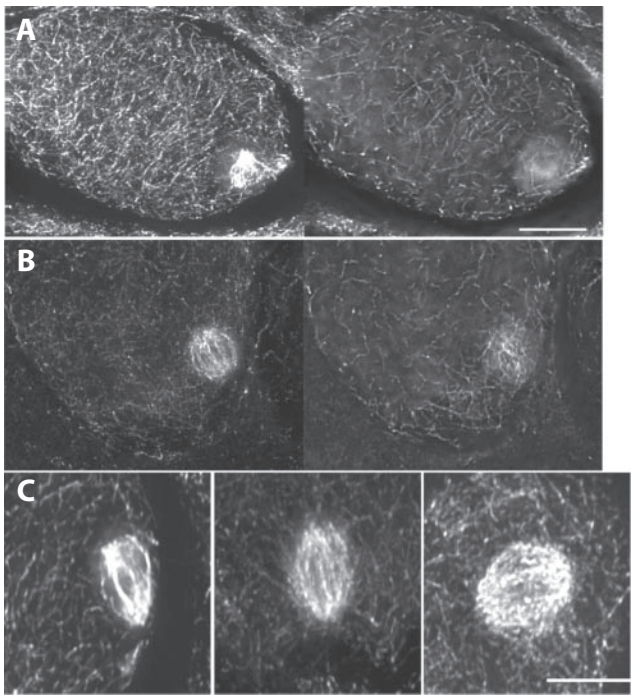

Figure 6. Microtubules extend between the spindle and cortex. (A and B) Deconvolved images of meiotic embryos fixed and stained with anti-tubulin antibodies show that cytoplasmic microtubules fill the embryos in all focal planes and extend to the cortex. (C) Deconvolved images of three different meiotic spindles stained with anti-tubulin antibodies show that cytoplasmic microtubules contact the spindle. Bars, 5 μm.

Cell Cycle Control of Cytoplasmic Dynein

The APC-dependent relocalization of dynein to spindle poles concomitant with APC-dependent and dynein-dependent late translocation initiation, suggests that dynein is activated by the APC. In one model of APC-activation of dynein, the diffuse localization of dynein throughout the spindle at metaphase would be the result of paused dynein molecules bound to microtubules through their motor domains. Activation of dynein's motor activity, perhaps through APC-dependent proteolysis of an inhibitor, would then result in minus-end–directed movement toward the spindle poles. Studies in budding yeast (Sheeman *et al*., 2003) indicate that active cytoplasmic dynein is cyclically targeted to a microtubule plus end before motoring toward

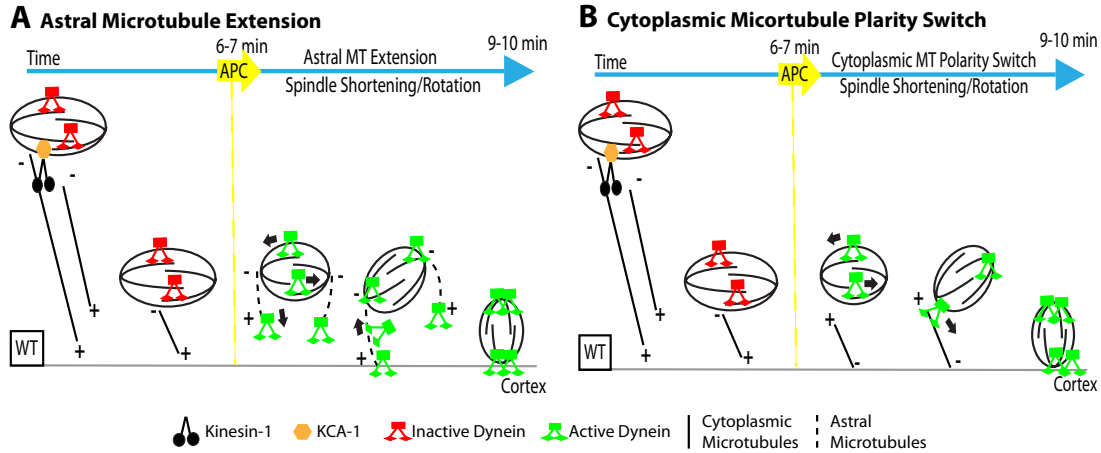

Figure 7. Models for the polarity paradox of the sequential action of kinesin-1 and cytoplasmic dynein during meiotic spindle positioning. In both models, the cytoplasmic microtubule array has microtubules with plus ends pointed toward the cortex with kinesin-1 bound to the spindle through KCA-1, pulling the spindle with a net pulling force toward the cortex. (A) On APC activation, inhibitors of dynein motility and/or astral microtubule growth are proteolyzed. Dynein would be transported on the growing plus ends of astral microtubules and be activated upon docking at a cortical site, where it would generate a cortical pulling force acting on spindle poles. (B) Alternatively, upon APC activation, microtubules are nucleated at the cortex resulting in a majority of cytoplasmic microtubules with minus ends pointed toward the cortex. Dynein at spindle poles would be attached to the spindle through the cargo-binding domain to allow the motor domains to interact with this new population of cytoplasmic microtubules.

the minus end. If, in *C. elegans*, activated dynein is targeted to plus ends of astral and spindle microtubules more slowly than it motors toward the minus end, this would explain the net concentration of dynein at meiotic spindle poles that occurs simultaneously with dynein-mediated late translocation.

Alternatively, APC activation may create binding sites for the cargo-binding domain of dynein at the spindle poles. This relocalization mechanism would be more compatible with dynein-mediated movement on cytoplasmic microtubules with minus ends oriented toward the cortex. Recent work indicates that accumulation of dynein heavy chain on meiotic spindles requires LIN-5, which in turn requires ASPM-1, which in turn requires calmodulin (van der Voet *et al*., 2009). This hierarchy, however, does not clearly distinguish between models of dynein relocalization after APC activation because the calmodulin/LIN-5/ASPM-1 complex might be required for dynein motor activity, for tethering dynein's cargo binding domain to the spindle, or both.

Independence of Kinesin-1 and Cytoplasmic Dynein

In several cases where kinesin-1 and cytoplasmic dynein act on the same cargo, their activities are interdependent. Inhibition of one motor reduces the activity of the other when they are both acting on peroxisomes, mitochondria or lipid droplets (Gross *et al*., 2000; Kural *et al*., 2005; Pilling *et al*., 2006). In the *C. elegans* meiotic embryo, cytoplasmic dynein moves one spindle pole toward the cortex with wild-type velocity even when kinesin-1 is inhibited with a mutation or by depletion of the essential regulator, KCA-1. Likewise, early, kinesin-1–dependent translocation is normal when cytoplasmic dynein is depleted by RNAi. Independence of kinesin-1 and cytoplasmic dynein makes sense when each motor is transporting the same cargo in the same direction on different subpopulations of microtubules to drive the unidirectional expulsion of chromosomes in polar bodies. This unidirectional transport contrasts with the continuous bidirectional transport between the neuronal cell body and the nerve terminal that is driven by the same motors.

ACKNOWLEDGMENTS

We thank Bruce Bowerman (University of Oregon), John White (University of Wisconsin-Madison), and Karen Oegema (University of California, San Diego) for strains; Lesilee Rose (University of California, Davis), Pierre Gönczy (Swiss Institute for Experimental Cancer Research), and John White for antibodies; and Jon Scholey, Joanne Engebrecht, Bo Liu, and Dan Starr for critical reading of the manuscript. This work was supported by National Institutes of Health National Institute of General Medical Sciences grant 1R01GM-079421 (to F.J.M.). M. E. was supported by National Institutes of Health training grant 5T32GM-007377.

REFERENCES

Baas, P. W., Deitch, J. S., Black, M. M., and Banker, G. A. (1988). Polarity orientation of microtubules in hippocampal neurons: uniformity in the axon and nonuniformity in the dendrite. Proc. Natl. Acad. Sci. USA *85*, 8335–8339.

Brenner, S. (1974). The genetics of *Caenorhabditis elegans*. Genetics *77*, 71–94.

Cha, B. J., Serbus, L. R., Koppetsch, B. S., and Theurkauf, W. E. (2002). Kinesin I-dependent cortical exclusion restricts pole plasm to the oocyte posterior. Nat. Cell Biol. *4*, 592–598.

DeBella, L. R., Hayashi, A., and Rose, L. S. (2006). LET-711, the *Caenorhabditis elegans* NOT1 ortholog, is required for spindle positioning and regulation of microtubule length in embryos. Mol. Biol. Cell *17*, 4911–4924.

Gassmann, R. *et al*. (2008). A new mechanism controlling kinetochore-microtubule interactions revealed by comparison of two dynein-targeting components: SPDL-1 and the Rod/Swilch?Zw10 complex. Genes Dev. *22*, 2385–2399.

Golden, A., Sadler, P. L., Wallenfang, M. R., Schumacher, J. M., Hamill, D. R., Bates, G., Bowerman, B., Seydoux, G., and Shakes, D. C. (2000). Metaphase to anaphase (mat) transition-defective mutants in *Caenorhabditis elegans*. J. Cell Biol. *151*, 1469–1482.

Gönczy, P., Pichler, S., Kirkham, M., and Hyman, A. A. (1999). Cytoplasmic dynein is required for distinct aspects of MTOC positioning, including centrosome separation, in the one cell stage *Caenorhabditis elegans* embryo. J. Cell Biol. *147*, 135–150.

Gönczy, P., Bellanger, J. M., Kirkham, M., Pozniakowski, A., Baumer, K., Phillips, J. B., and Hyman, A. A. (2001). ZYG-8, a gene required for spindle positioning in *C. elegans*, encodes a doublecortin-related kinase that promotes microtubule assembly. Dev. Cell *1*, 363–375.

Grava, S., Schaerer, F., Faty, M., Philippsen, P., and Barral, Y. (2006). Asymmetric recruitment of dynein to spindle poles and microtubules promotes proper spindle orientation in yeast. Dev. Cell *10*, 425–439.

Gross, S. P., Welte, M. A., Block, S. M., and Wieschaus, E. F. (2000). Dynein-mediated cargo transport in vivo. A switch controls travel distance. J. Cell Biol. *148*, 945–956.

Gupta, Jr., M. L., Carvalho, P., Roof, D. M., and Pellman, D. (2006). Plus end-specific depolymerase activity of Kip3, a kinesin-8 protein, explains its role in positioning the yeast mitotic spindle. Nat. Cell Biol. *8*, 913–923.

Kamath, R. S., Martinez-Campos, M., Zipperlin, P., Fraser, A. G., and Ahringer, J. (2000). Effectiveness of specific RNA-mediated interference through ingested double-stranded RNA in *Caenorhabditis elegans*. Genome Biol. 2, research0002.1-2.10.

Kirby, C., Kusch, M., and Kemphues, K. (1990). Mutations in the *par* genes of *Caenorhabditis elegans* affect cytoplasmic reorganization during the first cell cycle. Dev. Biol. *142*, 203–215.

Kural, C., Kim, H., Syed, S., Goshima, G., Gelfand, V. I., and Selvin, P. R. (2005). Kinesin and dynein move a peroxisome in vivo: a tug-of-war or coordinated movement? Science *308*, 1469–1472.

McCarter, J., Bartlett, B., Dang, T., and Schedl, T. (1999). On the control of oocyte meiotic maturation and ovulation in *Caenorhabditis elegans*. Dev. Biol. *205*, 111–128.

McNally, K., Audhya, A., Oegema, K., and McNally, F. J. (2006). Katanin controls mitotic and meiotic spindle length. J. Cell Biol. *175*, 881–891.

McNally, K., and McNally, F. J. (2005). Fertilization initiates the transition from anaphase I to metaphase II during female meiosis in *C. elegans*. Dev. Biol. *282*, 218–230.

Navara, C. S., First, N. L., and Schatten, G. (1994). Microtubule organization in the cow during fertilization, polyspermy, parthenogenesis, and nuclear transfer: the role of the sperm aster. Dev. Biol. *162*, 29–40.

O'Rourke, S. M., Dorfman, M. D., Carter, J. C., and Bowerman, B. (2007). Dynein modifiers in *C. elegans*: light chains suppress conditional heavy chain mutants. PLoS Genet. *3*, e128.

Park, D. H., and Rose, L. S. (2008). Dynamic localization of LIN-5 and GPR-1/2 to cortical force generation domains during spindle positioning. Dev. Biol. *315*, 42–54.

Praitis, V., Casey, E., Collar, D., and Austin, J. (2001). Creation of low-copy integrated transgenic lines in *Caenorhabditis elegans*. Genetics *157*, 1217–1226.

Pilling, A. D., Horiuchi, D., Lively, C. M., and Saxton, W. M. (2006). Kinesin-1 and Dynein are the primary motors for fast transport of mitochondria in *Drosophila* motor axons. Mol. Biol. Cell *17*, 2057–2068.

Shakes, D. C., Sadler, P. L., Schumacher, J. M., Abdolrasulnia, M., and Golden, A. (2003). Developmental defects observed in hypomorphic anaphase-promoting complex mutants are linked to cell cycle abnormalities. Development *130*, 1605–1620.

Sheeman, B., Carvalho, P., Sagot, I., Geiser, J., Kho, D., Hoyt, M. A., and Pellman, D. (2003). Determinants of *S. cerevisiae* dynein localization and activation: implications for the mechanism of spindle positioning. Curr. Biol. *13*, 364–372.

Shubeita, G. T., Tran, S. L., Xu, J., Vershinin, M., Cermelli, S., Cotton, S. L., Welte, M. A., and Gross, S. P. (2008). Consequences of motor copy number on the intracellular transport of kinesin-1-driven lipid droplets. Cell *135*, 1098–1107.

Skop, A. R., and White, J. G. (1998). The dynactin complex is required for cleavage plane specification in early *Caenorhabditis elegans* embryos. Curr. Biol. *8*, 1110–1116.

Tsou, M. F., Hayashi, A., DeBella, L. R., McGrath, G., and Rose, L. S. (2002). LET-99 determines spindle position and is asymmetrically enriched in response to PAR polarity cues in *C. elegans* embryos. Development *129*, 4469–4481.

Timmons, L., Court, D. L., Fire, A. (2001). Ingestion of bacterially expressed dsRNAs can produce specific and potent genetic interference in *Caenorhabditis elegans*. Gene *263*, 103–112.

van der Voet, M., Berends, C. W. H., Perreault, A., Nguyen-Ngoc, T., Gönczy, P., Vidal., M., Boxem, M., and van den Heuvel, S. (2009). NuMA-related LIN-5, ASPM-1, calmodulin and dynein promote meiotic spindle rotation independently of cortical LIN-5/GPR/Gα. Nat. Cell Biol. *11*, 269–277.

Yang, H. Y., Mains, P. E., and McNally, F. J. (2005). Kinesin-1 mediates translocation of the meiotic spindle to the oocyte cortex through KCA-1, a novel cargo adapter. J. Cell Biol. *169*, 447–457.

Yang, H. Y., McNally, K., and McNally, F. J. (2003). MEI-1/katanin is required for translocation of the meiosis I spindle to the oocyte cortex in *C. elegans*. Dev. Biol. *260*, 245–259.

Zhang, H., Skop, and A. R., White, J. G. (2008). Src and Wnt signaling regulate dynactin accumulation to the P2-EMS cell border in *C. elegans* embryos. J. Cell Sci. *15*, 155–161.